AFRL-RZ-WP-TP-2008-2258

FLUX PINNING IN $YBa_2Cu_3O_{7-\delta}$ THIN FILM SAMPLES LINKED TO STACKING FAULT DENSITY (POSTPRINT)

J. Wang, J.H. Kwon, J. Yoon, H. Wang, T.J. Haugan, F.J. Baca, N.A. Pierce, and P.N. Barnes

Power Generation Branch
Power Division

OCTOBER 2008

AIR FORCE RESEARCH LABORATORY
PROPULSION DIRECTORATE
WRIGHT-PATTERSON AIR FORCE BASE, OH 45433-7251
AIR FORCE MATERIEL COMMAND
UNITED STATES AIR FORCE

REPORT DOCUMENTATION PAGE

Form Approved
OMB No. 0704-0188

1. REPORT DATE *(DD-MM-YY)*	2. REPORT TYPE	3. DATES COVERED *(From - To)*
October 2008	Journal Article Postprint	

4. TITLE AND SUBTITLE

FLUX PINNING IN $YBa_2Cu_3O_{7-\delta}$ THIN FILM SAMPLES LINKED TO STACKING FAULT DENSITY (POSTPRINT)

5a. CONTRACT NUMBER
In-house

5b. GRANT NUMBER

5c. PROGRAM ELEMENT NUMBER
62203F

6. AUTHOR(S)

J. Wang, J.H. Kwon, J. Yoon, and H. Wang (Texas A&M University)
T.J. Haugan, F.J. Baca, N.A. Pierce, and P.N. Barnes (AFRL/RZPG)

5d. PROJECT NUMBER
3145

5e. TASK NUMBER
32

5f. WORK UNIT NUMBER
314532ZE

7. PERFORMING ORGANIZATION NAME(S) AND ADDRESS(ES)

Texas A&M University

Power Generation Branch (AFRL/RZPG)
Power Division
Air Force Research Laboratory, Propulsion Directorate
Wright-Patterson Air Force Base, OH 45433-7251
Air Force Materiel Command, United States Air Force

8. PERFORMING ORGANIZATION REPORT NUMBER
AFRL-RZ-WP-TP-2008-2258

9. SPONSORING/MONITORING AGENCY NAME(S) AND ADDRESS(ES)

Air Force Research Laboratory
Propulsion Directorate
Wright-Patterson Air Force Base, OH 45433-7251
Air Force Materiel Command
United States Air Force

10. SPONSORING/MONITORING AGENCY ACRONYM(S)
AFRL/RZPG

11. SPONSORING/MONITORING AGENCY REPORT NUMBER(S)
AFRL-RZ-WP-TP-2008-2258

12. DISTRIBUTION/AVAILABILITY STATEMENT

Approved for public release; distribution unlimited.

13. SUPPLEMENTARY NOTES

Journal article published in *Applied Physics Letters*, Vol. 92, 2008.

PAO Case Number: AFRL/WS 07-2244; Clearance Date: 24 Sep 2007.

14. ABSTRACT

In this paper, we report a strong correlation between the stacking fault (SF) density and the critical current density of $YBa_2Cu_3O_{7-\delta}$ (YBCO) thin films in applied field ($J_c^{\text{in-field}}$). We found that the $J_c^{\text{in-field}}$ ($H \| c$) increases as a clear linear dependence of the density of SF identified in the as-grown samples deposited on both $SrTiO_3$ (STO) and $LaAlO_3$ substrates. Detailed microstructural studies including cross-section transmission electron microscopy (TEM) and high resolution TEM were conducted for all the films deposited on STO substrates. This work suggests that the YBCO SF density plays an important role in the YBCO in-field transport performance.

15. SUBJECT TERMS

16. SECURITY CLASSIFICATION OF:			17. LIMITATION OF ABSTRACT:	18. NUMBER OF PAGES	19a. NAME OF RESPONSIBLE PERSON (Monitor)
a. REPORT	b. ABSTRACT	c. THIS PAGE			Lt. LaMarcus Hampton
Unclassified	Unclassified	Unclassified	SAR	10	19b. TELEPHONE NUMBER *(Include Area Code)* N/A

Standard Form 298 (Rev. 8-98)
Prescribed by ANSI Std. Z39-18

Flux pinning in $YBa_2Cu_3O_{7-\delta}$ thin film samples linked to stacking fault density

J. Wang,[1] J. H. Kwon,[1] J. Yoon,[1] H. Wang,[1,a)] T. J. Haugan,[2] F. J. Baca,[2] N. A. Pierce,[2] and P. N. Barnes[2]
[1]*Department of Electrical and Computer Engineering, Texas A&M University, College Station, Texas 77843-3128, USA*
[2]*Air Force Research Laboratory, Propulsion Directorate-Power Division, Wright-Patterson AFB, Ohio 45433-7251, USA*

(Received 23 October 2007; accepted 2 February 2008; published online 28 February 2008)

In this paper, we report a strong correlation between the stacking fault (SF) density and the critical current density of $YBa_2Cu_3O_{7-\delta}$ (YBCO) thin films in applied field ($J_c^{\text{in-field}}$). We found that the $J_c^{\text{in-field}}$ ($H\|c$) increases as a clear linear dependence of the density of SF identified in the as-grown samples deposited on both $SrTiO_3$ (STO) and $LaAlO_3$ substrates. Detailed microstructural studies including cross-section transmission electron microscopy (TEM) and high resolution TEM were conducted for all the films deposited on STO substrates. This work suggests that the YBCO SF density plays an important role in the YBCO in-field transport performance. © *2008 American Institute of Physics*. [DOI: 10.1063/1.2888749]

Recently, $YBa_2Cu_3O_{7-\delta}$ (YBCO) coated conductors are being scaled to commercial length for various applications.[1,2] A critical challenge is to maintain a high critical current density J_c as the YBCO coating is either made thicker or subjected to an external magnetic field.[3] One way is to enhance the YBCO flux pinning properties in both self-field and in field. For the in-field enhancement, nanoparticle doping of the YBCO matrix,[4,5] nanoparticle decoration at the YBCO growth interface,[6] rare earth mixtures in YBCO films,[7] and YBCO with minute dopants[8] were employed. For the self-field J_c enhancement, both the $YBCO/CeO_2$ multilayer approach[9] and the YBCO buffer layer optimization[10] were explored. It is believed that the defects introduced by these various approaches play an important role in enhancing the overall YBCO transport properties.[11] However, the exact mechanism(s) for the defect-related enhancements[12] in both the self-field J_c and the in-field J_c still remain unclear.

In this paper, we conducted a systematic study on the YBCO self-field and in-field transport properties [J_c^{sf} and $J_c^{\text{in-field}}$ ($H\|c$)] as a function of the microstructural characteristics of the samples. Detailed microstructural studies including cross-section transmission electron microscopy (TEM) and high resolution TEM were conducted on the films to view their microstructure. Using this information, we revealed a linear relation between the YBCO $J_c^{\text{in-field}}$ and the stacking fault (SF) density. The possible mechanisms and effects of the SF density on the YBCO transport property are proposed.

The depositions of YBCO films on $SrTiO_3$ (STO) and $LaAlO_3$ (LAO) substrates were performed by pulsed laser deposition (PLD) with a KrF excimer laser (Lambda Physik 305, $\lambda = 248$ nm, 4 Hz). Samples 1–4 were deposited at 775, 790, 800, and 825 °C, respectively. Different deposition temperatures were used to create the different defect densities identified in the samples. The O_2 pressure during deposition was 300 mTorr. The film thickness for all samples was about 300–350 nm. The YBCO films were characterized by measuring the critical transition temperature (T_c) and the J_c at liquid nitrogen temperature in both self-field and applied magnetic fields with a vibrating sample magnetometer (VSM) in a physical property measurement system by Quantum Design. Other experimental details of PLD processing and film characterization are described in Ref. 4 and references therein. Cross-sectional TEM (XTEM) studies on four representative samples on STO, including TEM and high resolution TEM (HRTEM), were performed with a Philips CM200 analytical electron microscope with point-to-point resolution of 0.21 nm.

Figure 1 shows the critical current density as a function of the applied magnetic field ($J_c^{\text{in-field}}$ measured at both 65 and 77 K, $H\|c$) for YBCO samples 1–4 deposited at different temperatures. It clearly shows that, for the whole field range

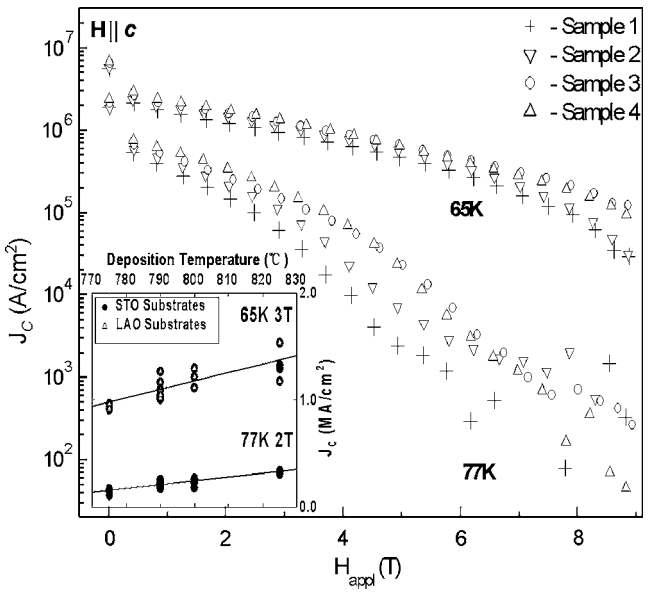

FIG. 1. The plot of $J_c^{\text{in-field}}$ vs H ($H\|c$) for samples 1–4 deposited at different temperatures and J_c measured by VSM. The inset shows $J_c^{\text{in-field}}$ (77 K at 2 T and 65 K at 3 T) vs deposition temperature for samples deposited on both STO and LAO substrates.

a)Electronic mail: wangh@ece.tamu.edu.

0003-6951/2008/92(8)/082507/3/$23.00

TABLE I. Microstructural and transport data for the samples (1–4).

Sample No.	Deposit temp. (°C)	Thickness (μm)	$J_c^{\text{in-field}}$ (MA/cm^2) at 65 K, 3T	J_c^{sf} (MA/cm^2) at 77 K	SF density (10^6/cm) Area 1	SF density (10^6/cm) Area 2	Average SF density (10^6/cm)
1	775	0.32	0.94	2.22	0.41	0.55	0.48
2	790	0.31	1.02	2.19	0.55	0.62	0.59
3	800	0.34	1.12	2.20	0.65	0.80	0.73
4	825	0.35	1.30	2.63	1.06	1.18	1.12

(0–9 T), the samples deposited at the different temperatures show different in-field performance, especially in the high field regime. The J_c^{sf} is about the same for all samples (see J_c^{sf} values in Table I). In order to view the $J_c^{\text{in-field}}$ variation trend clearly, we plot the $J_c^{\text{in-field}}$ (at 65 K, 3 T and 77 K, 2 T for samples deposited on both STO and LAO substrates) as a function of the deposition temperature (shown as inset in Fig. 1). For the 65 K, 3 T data on STO substrates, the $J_c^{\text{in-field}}$ increased from 0.94 MA/cm^2 to a maximum of 1.3 MA/cm^2, following a linear relation. A clear linear trend was observed for the 77 K, 2 T data, as well as the data on LAO substrates at both 77 and 65 K. Having established a series of samples with varying in-field properties although similar self-field values, it will be easier to link differences in the microstructural characteristics of the YBCO to their effectiveness as in-field pinning centers. Microscopy was now used to determine what the precise effect on the YBCO was to cause this variation in transport property.

To resolve which defect(s) could be responsible for the observed $J_c^{\text{in-field}}$ temperature dependence, we conducted a detailed microstructure study including XTEM and HRTEM on four of the YBCO films deposited on the STO substrates. A possible explanation of the observed $J_c^{\text{in-field}}$ deposition temperature dependence is that the epitaxial quality of the YBCO thin films improves as the deposition temperature increases, and, thus providing a better transport property. However, in applied fields, as opposed to self-field, pinning centers are critical to prevent flux flow to maintain higher J_c, suggesting that the in-field performance largely depends on the defects in the YBCO films which act as effective flux pinning centers[13] since no foreign material is being added or no alternate structure is being imposed. These defects could include misfit dislocations, edge and screw dislocations,[14] grain boundaries,[15] low angle domain boundaries, antiphase boundaries, twins, and SFs.[16,17] Figures 2(a)–2(d) show the XTEM images of YBCO films (Nos. 4, 3, 2, and 1) on STO substrates deposited at 825, 800, 790, and 775 °C, respectively. All images were taken at the same image conditions, i.e., the same magnification and the same objective aperture, to ensure a fair comparison. All four samples have grown as high quality epitaxial thin film on STO substrate with clear and straight lattices observed. The film/substrate interfaces remain clear without any obvious indication of interfacial reactions for all samples. Selected area diffraction patterns for all samples (not shown here) showed the distinguished diffractions from YBCO films, which suggests that these films have comparable film quality.

One type of defect observed in all four YBCO films is a high density of SFs. The SF is one kind of the commonly observed defects in YBCO. It is caused by the absence of or additional atomic planes during the thin film growth.[3] We conducted a detailed analysis on the SF densities for all HRTEM images (with an average area of 0.25×0.25 μm^2) taken for all four samples. For each sample, at least two HRTEM images were analyzed and averaged for the overall SF density. The data from the inset in Fig. 1 essentially show the larger data set which the table represents since the SF density directly varied due to the deposition temperature. The SFs in the view area were marked as white arrows. There are two types of SFs in the images. One type shows as a clear straight line across the view area (marked as a solid white arrow, counted as one SF). The other type shows as a discontinuous SF in the view area (marked as a dashed arrow, counted as a half SF). Table I lists the details of the samples in this study including the $J_c^{\text{in-field}}$ values, the SF densities for the two view areas, and the average SF densities.

The average density of YBCO SF varies from 4.8×10^5/cm to 1.12×10^6/cm as the deposition temperature increases from 775 to 825° °C. Figure 3 shows the plot of SF density as a function of the $J_c^{\text{in-field}}$ acquired both at 65 K and $H\|c=3$ T and at 77 K and $H\|c=2$ T. It is interesting to note that a clear linear relation is observed between the SF

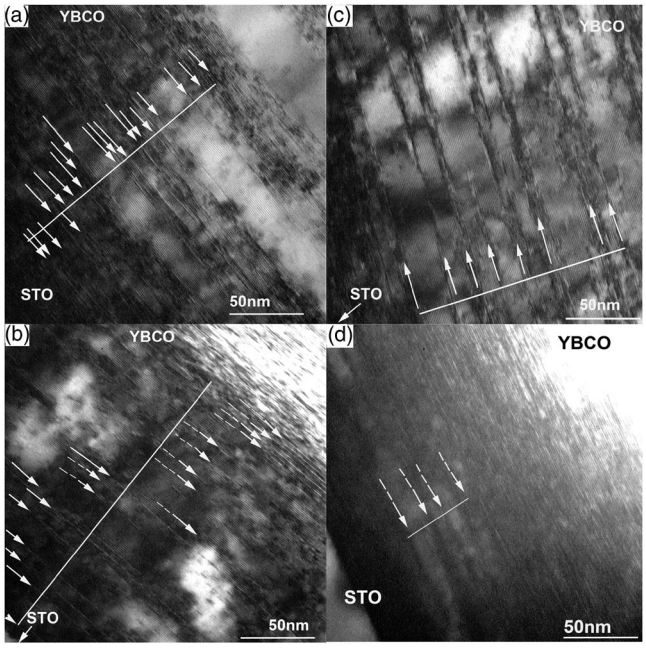

FIG. 2. XTEM images of YBCO samples 4, 3, 2, and 1 on STO substrates deposited at (a) 825 °C, (b) 800 °C, (c) 790 °C, and (d) 775 °C, respectively. High density SFs are clearly observed in all four samples and marked as white arrows. (The vertical lines in the images are used for visual guide.)

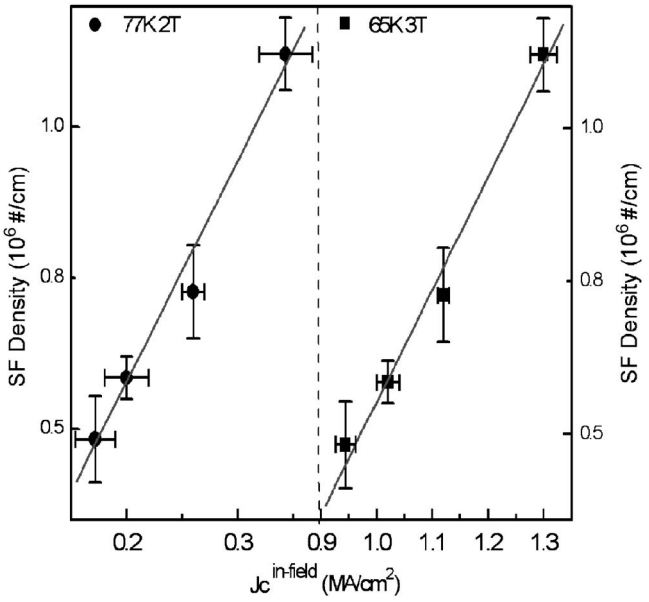

FIG. 3. The plot of SF density as a function of $J_c^{\text{in-field}}$ ($H\|c$) at 65 K, 3 T and at 77 K, 2 T for the samples on STO substrate. A clear linear relation is observed between the SF density and the $J_c^{\text{in-field}}$.

density and the $J_c^{\text{in-field}}$ ($H\|c$) for both measurement temperatures. Again, note that these four points are representative of a much larger data set. This suggests that the SF density has a strong effect on the in-field performance and may be primarily responsible for the increase of $J_c^{\text{in-field}}$. It is interesting that J_c ($H\|c$) increase was observed, as compared to other studies with maximum operating depth Metal-organic Deposition (MOD) films where an increase of J_c ($H\|ab$) was closely correlated with SF defects.[17] As mentioned above, the SFs are formed by the absence of or additional planes during the thin film growth. The terminating point of the SF at the grain boundaries can be essentially considered as the dislocation core of a pure edge dislocation. The dislocation core region is a highly defective region where the strain in the core region can possibly introduce lattice distortion as well as cation disorder. The linear density of the SF can also be considered as misfit dislocation density along the *c*-axis direction. These high density SFs can potentially act as strong *c*-axis pinning centers in the PLD YBCO films with a large amount of columnar grain boundaries, and therefore the higher SF density results in higher $J_c^{\text{in-field}}$ ($H\|c$) in the samples deposited at a higher temperature. In MOD films, the SF pinning effects along the *c* axis might not be strong due to the films being laminar with grain boundaries that meander in the thin planar lamina with different physical structures than SFs.[18] This meandering in the plane correlates to increased *ab* pinning but does not enhance *c*-axis pinning.

In conclusion, high quality YBCO thin films were deposited on STO and LAO substrates at various temperatures to vary the density of microstructural defects. The samples show varying in-field performance ($J_c^{\text{in-field}}$, $H\|c$, up to 9 T) in all field ranges while the J_c^{sf} remains relatively constant. As representative data, the $J_c^{\text{in-field}}$ plots for 65 K, 3 T and 77 K, 2 T were presented. Detailed SF analysis was conducted and provided a clear linear relation between the SF density and the $J_c^{\text{in-field}}$ ($H\|c$) value. It is suggested that the terminating point of the two-dimensional planar defects can introduce additional defects in the *c*-axis direction, and therefore enhance the in-field performance of J_c ($H\|c$). Differences in the effects of the SF density between the columnar growth of PLD films and laminar MOD films suggest that defect induced pinning mechanisms must consider the film growth and not just the defect itself.

This research was funded by the Air Force Office of Scientific Research (Contract No. FA9550-0701-0108), AFOSR summer faculty program, and AFRL, Propulsion Directorate.

[1] D. Larbalestier, A. Gurevich, D. M. Feldmann, and A. Polyanskii, Nature (London) **414**, 368 (2001).
[2] P. N. Barnes, M. D. Sumption, and G. L. Rhoads, Cryogenics **45**, 670 (2005).
[3] S. R. Foltyn, L. Civale, J. L. MacManus-Driscoll, Q. X. Jia, B. Maiorov, H. Wang, and M. Maley, Nat. Mater. **6**, 631 (2007).
[4] T. Haugan, P. N. Barnes, R. Wheeler, F. Meisenkothen, and M. Sumption, Nature (London) **430**, 867 (2004).
[5] S. Kang, A. Goyal, J. Li, A. A. Gapud, P. M. Martin, L. Heatherly, J. R. Thompson, D. K. Christen, F. A. List, M. Paranthaman, and D. F. Lee, Science **311**, 1911 (2006).
[6] T. Aytug, M. Paranthaman, A. A. Gapud, S. Kang, M. Varela, P. M. Martin, J. M. Raitano, S.-W. Chan, J. R. Thompson, and D. K. Christen, IEEE Trans. Appl. Supercond. **17**, 3720 (2007).
[7] J. L. MacManus-Driscoll, S. R. Foltyn, Q. X. Jia, H. Wang, A. Serquis, B. Maiorov, L. Civale, Y. Lin, M. E. Hawley, M. P. Maley, and D. E. Peterson, Appl. Phys. Lett. **84**, 5329 (2004).
[8] P. N. Barnes, J. W. Kell, B. C. Harrison, T. J. Haugan, C. V. Varanasi, M. Rane, and F. Ramos, Appl. Phys. Lett. **89**, 012503 (2006).
[9] S. R. Foltyn, H. Wang, L. Civale, Q. X. Jia, P. N. Arendt, B. Maiorov, Y. Li, M. P. Maley, and J. L. MacManus-Driscoll, Appl. Phys. Lett. **87**, 162505 (2005).
[10] H. Wang, S. R. Foltyn, P. N. Arendt, Q. X. Jia, J. L. MacManus-Driscoll, X. Zhang, and P. C. Dowden, J. Mater. Res. **19**, 1869 (2004).
[11] L. Civale, B. Maiorov, A. Serquis, J. O. Willis, J. Y. Coulter, H. Wang, Q. X. Jia, P. N. Arendt, J. L. MacManus-Driscoll, M. P. Maley, and S. R. Foltyn, Appl. Phys. Lett. **84**, 2121 (2004).
[12] J. Gutierrez, A. Llordes, J. Gazquez, M. Gibert, N. Roma, A. Pomar, F. Sandiumenge, N. Mestres, T. Puig, and X. Obradors, Nat. Mater. **6**, 367 (2007).
[13] K. Matsumoto, T. Horide, A. Ichinose, S. Horii, Y. Yoshida, and M. Mukaida, Jpn. J. Appl. Phys., Part 2 **44**, L246 (2005).
[14] B. Dam, J. M. Huijbregtse, F. C. Klaassen, R. C. F. van der Geest, B. Doornbos, J. H. Rector, A. M. Testa, S. Freisem, J. C. Martinez, B. Stauble-Pumpin, and R. Griessen, Nature (London) **399**, 439 (1999).
[15] D. T. Verebelyi, D. K. Christen, R. Feenstra, C. Cantoni, A. Goyal, D. F. Lee, M. Paranthaman, P. N. Arendt, R. F. DePaula, J. R. Groves, and C. Prouteau, Appl. Phys. Lett. **76**, 1755 (2000).
[16] S. I. Kim, F. Kameain, Z. Chen, A. Gurevich, D. C. Larbalestier, T. Haugan, and P. Barnes, Appl. Phys. Lett. **90**, 252502 (2007).
[17] E. D. Specht, A. Goyal, J. Li, P. M. Martin, X. Li, and M. W. Rupich, Appl. Phys. Lett. **89**, 162510 (2006).
[18] D. M. Feldmann, T. G. Holesinger, C. Cantoni, R. Feenstra, N. A. Nelson, D. C. Larbalestier, D. T. Verebelyi, X. Li, and M. Rupich, J. Mater. Res. **21**, 923 (2006).